The budget and partitioning of stratospheric chlorine during the 1997 Arctic summer

B. Sen,[1] G. B. Osterman,[1] R. J. Salawitch,[1] G. C. Toon,[1] J. J. Margitan,[1] J.-F. Blavier,[1] A. Y. Chang,[1] R. D. May,[1] C. R. Webster,[1] R. M. Stimpfle,[2] G. P. Bonne,[2] P. B. Voss,[2] K. K. Perkins,[2] J. G. Anderson,[2] R. C. Cohen,[3] J. W. Elkins,[4] G. S. Dutton,[4,5] D. F. Hurst,[4,5] P. A. Romashkin,[4,5] E. L. Atlas,[6] S. M. Schauffler,[6] M. Loewenstein[7]

Short title: STRATOSPHERIC CHLORINE DURING THE 1997 ARCTIC SUMMER

[1]Jet Propulsion Laboratory, California Institute of Technology, Pasadena, CA

[2]Harvard University, Cambridge, MA

[3]University of California, Berkeley, CA

[4]NOAA/CMDL, Boulder, CO

[5]CIRES, CU, Boulder, CO

[6]NCAR, Boulder, CO

[7]NASA AMES Research Center, Moffett Field, CA

Abstract. Volume mixing ratio profiles of HCl, HOCl, $ClNO_3$, CH_3Cl, CFC-12, CFC-11, CCl_4, HCFC-22, and CFC-113 were measured simultaneously from 9 to 38 km by the Jet Propulsion Laboratory MkIV Fourier Transform Infrared solar absorption spectrometer during two balloon flights from Fairbanks, Alaska (64.8°N) on 8 May and 8 July 1997. The altitude variation of total organic chlorine (CCl_y), total inorganic chlorine (Cl_y), and the nearly constant value (3.7±0.2 ppbv) of their sum (Cl_{TOT}) demonstrates that the stratospheric chlorine species available to react with O_3 are supplied by the decomposition of organic chlorinated compounds whose abundances are well quantified. Measured profiles of HCl and $ClNO_3$ agree well with photochemical model values (differences < 10% for altitudes below 34 km), particularly when production of HCl by ClO+OH is included in the model. Our results demonstrate that the production of HCl by ClO + OH plays a small role (< 5%) in the partitioning of HCl and $ClNO_3$ for the sampled air masses for altitudes below ~28 km because the concentration of ClO is suppressed during summer at high latitudes. Both the measured and calculated $[ClNO_3]/[HCl]$ ratios exhibit the expected near linear variation with $[O_3]^2/[CH_4]$ over a broad range of altitudes. MkIV measurements of HCl, $ClNO_3$, and CCl_y agree well with ER-2 *in situ* observations of these quantities for directly comparable air masses. These results demonstrate good understanding of the budget of stratospheric chlorine and that the partitioning of inorganic chlorine is accurately described (differences < 10%) by photochemical models that employ JPL97 reaction rates for the environmental conditions encountered: relatively warm temperatures, long periods of solar illumination, and relatively low aerosol surface areas.

1. Introduction

We report MkIV profiles of stratospheric chlorine gases obtained during balloon flights on 8 May and 8 July 1997 from Fairbanks, Alaska (64.8°N, 147.6°W) during the Photochemistry of Ozone Loss in the Arctic Region in Summer (POLARIS) campaign. Analysis of these observations tests our understanding of the stratospheric chlorine budget through its organic (CCl_y = 2·CFC-12 + 3·CFC-11 + 3·CFC-113 + 4·CCl_4 + CH_3Cl + HCFC-22 + 3·CH_3CCl_3) and inorganic (Cl_y = HCl + $ClNO_3$ + HOCl + ClO) components. Observations of HCl, $ClNO_3$, various CCl_y gases, and N_2O obtained *in situ* by instruments on board the NASA ER-2 aircraft during POLARIS provide a valuable opportunity for comparison of the abundance of these species acquired by vastly different measurement techniques. A photochemical model is also used to assess the impact of the different environmental conditions sampled by MkIV and the ER-2 on the comparisons of HCl vs. N_2O and $ClNO_3$ vs. N_2O.

1.1. MkIV Interferometer

The MkIV Fourier Transform Infrared (FTIR) spectrometer [*Toon*, 1991] obtains remote measurements of the composition of the atmosphere using the solar occultation technique. The brightness and stability of the Sun allow high signal-to-noise ratio spectra with broad coverage (650-5650 cm^{-1}) to be obtained at high spectral resolution (0.01 cm^{-1}), allowing the abundances of a large number of gases to be measured simultaneously, including O_3, N_2O, CH_4, HCl, HOCl, $ClNO_3$, CH_3Cl, CFC-12, CFC-11, CCl_4, HCFC-22, and CFC-113. Very long absorption paths through the atmosphere are obtained by viewing the rising or setting Sun, yielding high sensitivity to these trace species. From a series of such spectra measured at different tangent altitudes the volume mixing ratio (vmr) profiles of these gases are retrieved, as described by *Sen et al.* [1996, 1998].

The measurement precision is calculated during the retrieval process and is based on factors such as residuals in spectral fitting. In general, gases with numerous, strong, well-isolated spectral lines (e.g., O_3, NO_2, and HCl) yield precisions in their retrieved vmr of typically ~5% of the peak vmr value. The estimated 1σ uncertainties in the accuracy of the spectroscopic parameters used in the vmr retrievals are 6% for O_3, 5% for N_2O and HCl, 10% for CFC-12, CFC-11, CCl_4, and HCFC-22, 15% for $ClNO_3$ and CH_3Cl, and 20% for CFC-113 and HOCl [*Abrams et al.*, 1996b; *Brown et al.*, 1996]. Other systematic error terms such as tangent pressure and temperature uncertainties are thought to be negligible (< 3%). Tangent pressures have been retrieved using temperature insensitive CO_2 lines, and tangent temperatures were retrieved using temperature sensitive CO_2 lines. *Abrams et al.* [1996a] have shown that the uncertainties in the tangent pressure and tangent temperature retrieved by the Atmospheric Trace

Molecule Spectroscopy (ATMOS) instrument, which uses a measurement and data analysis technique similar to MkIV, are typically 1 to 3%, limited by our knowledge of the vmr profile of CO_2 and uncertainties in its spectroscopy. Retrievals of the vmr profile of N_2 (not shown) confirm that the viewing geometry and atmospheric conditions (i.e., pressure, temperature) have been calculated accurately (see *Abrams et al.* [1996a] for a related discussion of ATMOS retrievals of N_2). The error bars used in the figures for all the MkIV observations reported here represent the 1σ measurement precision. *Toon et al.* [1999a] show, based on a comparison of MkIV observations during POLARIS and measurements acquired by ER-2 instruments that are closely located in space and time, that the remote and *in situ* vmr profiles of O_3, N_2O, H_2O (above 17 km), and CFC-12 agree to better than 5%. The MkIV and ER-2 profiles of CH_4, CO, HCl, $ClNO_3$, NO_y, and CFC-11 are shown to agree to within 10%, whereas profiles for CFC-113 and CCl_4 exhibit differences as high as 15% [*Toon et al.*, 1999a]. This study and an earlier intercomparison of ATMOS and ER-2 observations [*Chang et al.*, 1996] demonstrate the ability to combine remote and *in situ* measurements for quantifying the budget and partitioning of stratospheric chlorine.

1.2. ER-2 *In Situ* Instruments

Several instruments on board the ER-2 provide simultaneous *in situ* measurements of $ClNO_3$, HCl, N_2O, and CCl_y. The abundance of $ClNO_3$ was measured by thermally dissociating it to ClO and NO_2. The resonant fluorescence detection of Cl (formed by titrating ClO with NO) allows measurements of $ClNO_3$ with a 1σ precision and accuracy of 10 pptv and 20%, respectively [*Bonne et al.*, 1999].

In situ vmrs of HCl were obtained with a 1σ precision of 0.07 ppbv and an accuracy of 10% by the ALIAS (Aircraft Laser Infrared Absorption Spectrometer) tunable diode laser instrument [*Webster et al.*, 1994] using spectral transitions common to MkIV. Another tunable diode laser instrument on board the ER-2 aircraft, ATLAS (Airborne Tunable Laser Absorption Spectrometer), measures N_2O by monitoring absorption at 2230 cm^{-1}, at a sampling rate of 1 Hz, with a 1σ total uncertainty of 3% [*Loewenstein et al.*, 1989].

The vmrs of CFC-11, CFC-113, CH_3CCl_3, CCl_4, and CFC-12 were measured with 1σ precisions and accuracies of better than 2% and 4%, respectively, by the ACATS-IV (Airborne Chromotograph for Atmospheric Trace Species) instrument [*Elkins et al.*, 1996]. The precision and accuracy of $CHCl_3$ measurements during POLARIS is estimated to be about 10% and 15%, respectively. The gases are measured in one of four separate chromotographic channels, each incorporating an electron capture detector, at intervals of either 125 s or 250 s (N_2O, SF_6). During flights, the instrument is calibrated once every 625 s (1250 s for N_2O and SF_6) by injecting a dried, whole

air standard with approximately 80% of the tropospheric mixing ratio of each species. Observations of HCFC-22 and CH_3Cl (gases required to define CCl_y and not measured by ACATS) were obtained with 1σ precision and accuracies of better than 3% and 7%, respectively, by analysis of air collected by a Whole Air Sampler (WAS) system on board the ER-2 [*Schauffler et al.*, 1993].

1.3. Photochemical Model

A photochemical model used in many previous stratospheric studies [e.g., *Salawitch et al.*, 1994a, b; *Michelsen et al.*, 1996; *Sen et al.*, 1998; *Osterman et al.*, 1999] was used to interpret the MkIV and ER-2 observations. The abundances of radical (i.e., NO, NO_2, OH, HO_2, ClO, and BrO) and reservoir (i.e., HNO_3, HCl, N_2O_5, and $ClNO_3$) gases were calculated allowing for diurnal variation and assuming a balance between production and loss rates of each species integrated over a 24-hour period, for the latitude and temperature of the observations. Concentrations of precursors (i.e., O_3, H_2O, CH_4, CO, and C_2H_6), the total abundance of NO_y, and the sum HCl + $ClNO_3$ + HOCl were constrained to match observations of MkIV. The input O_3 and temperature profiles are taken from MkIV observations up to balloon float altitude (38 km). For higher altitudes, climatological O_3 and temperature profiles from *Keating and Young* [1985] were used, updated to represent more recent observations [G. Keating, NASA Langley, private communication, 1994]. The abundance of Br_y was specified based on its correlation with N_2O [*Wamsley et al.*, 1998]. Photolysis rates are found using a radiative transfer model that accounts for Rayleigh scattering [*Prather*, 1981] and the geometry of the direct beam at high solar zenith angles [*Salawitch et al.*, 1994b]. Reaction rates and absorption cross sections were adopted from *DeMore et al.* [1997], unless noted otherwise.

All heterogeneous reactions on sulfate aerosols believed to affect partitioning of stratospheric gases at high latitudes were included in the model. Reaction probabilities for heterogeneous hydrolysis of N_2O_5 (γ=0.1) and $BrNO_3$ (γ=0.8) originate from *DeMore et al.* [1997]. The reaction probability for HONO + HCl (γ=0.02) measured by *Zhang et al.* [1996] was used. The formulations of *Ravishankara and Hanson* [1996] were used for the sulfate heterogeneous reactions $ClNO_3$ + HCl and $ClNO_3$ + H_2O. Kinetic parameters used for the heterogeneous reactions of HOCl + HCl and HOBr + HCl are from *Donaldson et al.* [1997]. Profiles of aerosol surface area originate from zonal, monthly mean observations of SAGE II [*Thomason et al.*, 1997] for 65°N, May and July 1997 and are typical of background (i.e., non-volcanic) conditions [L.W. Thomason, NASA Langley, private communication, 1998]. Although heterogeneous reactions involving HCl and $ClNO_3$ on sulfate aerosols have been included in our analysis, they have no effect on the model results due to the warm temperatures associated with the

observations.

2. Results and Discussions

2.1. Chlorine Budget

Our understanding of the budget of chlorine-bearing gases can be tested in a simple manner owing to the long lifetime of Cl_y and the nearly complete conversion of the organic chlorinated source molecules to Cl_y species (i.e., within 6 years of entering the stratosphere). Testing the budget of stratospheric chlorine involves the measurement of concentrations of a large number of Cl-bearing species, which must presently be achieved by combining measurements of several different techniques. The broad spectral coverage of the MkIV FTIR allows most organic and inorganic chlorine species to be measured simultaneously for the same air mass. MkIV measures nearly all of the CCl_y gases that significantly contribute to the organic budget (CFC-12, CFC-11, CFC-113, CCl_4, CH_3Cl, and HCFC-22) [*Sen et al.*, 1996], and three of the major Cl_y species (HCl, HOCl, and $ClNO_3$). The only principal species not measurable by MkIV are CH_3CCl_3 and ClO. The profile of CH_3CCl_3 used here was estimated using CFC-12 measured by MkIV and the correlation of CH_3CCl_3 with CFC-12 measured by ACATS; CH_3CCl_3 makes a maximum contribution of $\sim$8% to CCl_y. Measurements of other organic chlorinated compounds obtained by surface flask network [*Kaye et al.*, 1994, Chapter 1] show that the combined organic chlorine content not measured by MkIV is less than 100 pptv (< 3%). Sunrise profiles of ClO calculated using the photochemical model were added to the measured vmrs of HCl, $ClNO_3$, and HOCl to determine Cl_y. The contribution of calculated ClO to Cl_y is never larger than 8% for the high latitude summer air masses sampled by MkIV.

Figure 1 illustrates the altitude variation of CCl_y and Cl_y as well as their sum Cl_{TOT} measured by MkIV during sunrise on 8 May 1997. The near constant value for Cl_{TOT} of 3.7$\pm$0.2 ppbv between 9 and 38 km confirms quantitatively that anthropogenic organic gases are converted into stratospheric inorganic chlorine. The fact that Cl_y goes to zero near 9 km (the local tropopause based on the retrieved temperature and H_2O profile) confirms that CCl_y species are the dominant source of stratospheric Cl_y and that stratospherically significant amounts of Cl_y are not present at the high latitude tropopause during summer. The local maximum in Cl_y near 12 km (mirrored in CCl_y) is consistent with a small "fold" in N_2O and CH_4 observed by MkIV and appears to be a robust feature of the Arctic lower stratosphere during early May 1997, since similar behavior was observed on numerous occasions by ER-2 instruments [e.g., *Toon et al.*, 1999b]. The value of Cl_{TOT} agrees with estimates derived from the surface flask network for the average for 1991–1996 [*Kaye et al.*, 1994, Chapter 1] and the findings of *Zander et al.* [1996] based on analyses of measurements made by ATMOS during November

1994 at mid-latitudes. The mean age of stratospheric air is approximately 5 years in the mid-stratosphere [*Boering et al.*, 1996] and during POLARIS ranged from a few months to 4 years at 20 km based on *in situ* measurements of CO_2 [A.E. Andrews, Harvard University, private communication, 1998] to nearly 6 years at 38 km based on MkIV measurements of fluorine-bearing source gases and HF.

Figure 1.

It is unclear whether the apparent altitude variations of Cl_{TOT} are present in the atmosphere or are measurement artifacts. All points of the stratospheric profile of Cl_{TOT} derived from the MkIV data lie within the interval 3.7±0.2 ppbv (except perhaps the highest and lowest altitude points, whose error bars are large but do overlap this interval). There is some structure in the profile of Cl_{TOT}, with a broad maximum of ~3.9 ppbv between 24 and 27 km and a decrease above 34 km that drops below the 3.7 ppbv average. Since the tropospheric burden of CCl_y has been nearly constant (but slightly declining at ~1% yr^{-1} after 1994) for the past 5 years [*Montzka et al.*, 1996] and upper stratospheric air is ~6 years old, we would not expect a significant variation of Cl_{TOT} due to the age of air. It is unlikely that the altitude variation of Cl_{TOT} above 30 km is due to gross errors in calculated ClO, based on comparisons with balloon-borne measurements of ClO during Arctic spring obtained by the Submillimeter Limb Sounder (SLS) instrument on 30 April 1997 [R. Stachnik, JPL, private communication, 1998]. Our photochemical calculations using standard chemistry demonstrate that the other Cl_y species not measured by MkIV (e.g., Cl, Cl_2, Cl_2O_2, etc.) contribute less than 1% to Cl_{TOT} in the 8 to 38 km altitude range and therefore are unlikely to be responsible for the apparent altitude variation of Cl_{TOT}. *Jaeglé et al.* [1996] suggested that $HClO_4$ could contribute significantly to the budget of Cl_{TOT} in the lower stratosphere based on an analysis of MkIV observations obtained at 35°N during September 1993 under conditions of volcanically perturbed aerosol loading. However, we believe it is unrealistic to ascribe the local minimum of Cl_{TOT} near 15 km to the presence of $HClO_4$ because aerosol concentrations were considerably smaller during POLARIS than those prevalent during September 1993. Furthermore, *Abbatt* [1996] reported laboratory measurements of the uptake coefficient for ClO on sulfate aerosols that were approximately a factor of 10 smaller than the value used in the model calculations of *Jaeglé et al.* [1996]. It is possible that some of the apparent variation in Cl_{TOT} below 15 km is caused by a bias in the MkIV retrieval of CCl_4 that is revealed based on comparison with ACATS observations of this gas described in Section 2.2.2.

2.2. Chlorine Partitioning

2.2.1. MkIV Balloon Measurements Observed and calculated profiles of HCl and $ClNO_3$ for the two MkIV flights are shown in Figure 2. Two sets of calculations are shown: one assumes that the reaction of ClO + OH has a 0% yield for HCl, while the

other assumes a temperature dependent yield for HCl (i.e, ~5% at 298 K to ~6% at 210 K) based on the *Lipson et al.* [1997] study of ClO + OD. In contrast to simulations for observations obtained at either lower latitudes or high latitudes during winter [e.g., *Minschwaner et al.*, 1993; *Chance et al.*, 1996; *Michelsen et al.*, 1996], during Arctic summer calculated vmrs of $ClNO_3$ and HCl are relatively insensitive to production of HCl from ClO + OH at altitudes where concentrations of ClO are suppressed due to high abundances of NO_x (below 28 km in May and below 32 km in July). The increased apportionment of NO_y species into NO_x during Arctic summer is clear from MkIV observations of the NO_x/NO_y ratio in May and July 1997 [*Osterman et al.*, 1999].

The results shown in Figure 2 demonstrate a good understanding of the photochemical processes that regulate the partitioning of HCl and $ClNO_3$, the dominant components of Cl_y, for the summer high latitude stratosphere. There is good agreement between the profiles of HCl and $ClNO_3$ measured by MkIV and those calculated with the *Lipson et al.* [1997] temperature dependent yield of HCl from the reaction of ClO + OH. However, the only notable disagreement [e.g., differences larger than the total uncertainty, accuracy + precision, of the MkIV measurement] between the observed profiles and those calculated using a HCl yield of 0% occurs above 34 km for the 8 May 1997 balloon flight. Even though the effect of including production of HCl from ClO + OH in the model is small, the MkIV measurements indicate the need for an additional source of HCl in the model when 0% yield is assumed. These comparisons provide additional evidence that ClO + OH → HCl is indeed the correct explanation for the discrepancies in the $ClNO_3$/HCl ratio previously noted by numerous analyses of mid-latitude and tropical observations [e.g., *Minschwaner et al.*, 1993; *Chance et al.*, 1996; *Michelsen et al.*, 1996].

Figure 2.

It is instructive to examine the processes that regulate the $ClNO_3$/HCl ratio to better understand the good agreement between measured and calculated vmrs of $ClNO_3$ and HCl. Balancing the gas phase sources and sinks of $ClNO_3$ and HCl leads to the following expressions:

$$[ClNO_3] = \frac{k_{ClO+NO_2;M}\langle ClO\cdot NO_2\rangle}{J_{ClNO_3}} = \epsilon\,\frac{k_{ClO+NO_2;M}\langle ClO\rangle\langle NO_2\rangle}{J_{ClNO_3}}, \quad (1a)$$

$$[HCl] = \frac{k_{Cl+CH_4}\langle Cl\rangle[CH_4]+k_{Cl+C_2H_6}\langle Cl\rangle[C_2H_6]+Y\cdot k_{ClO+OH}\langle ClO\cdot OH\rangle+k_{Cl+HO_2}\langle Cl\cdot HO_2\rangle}{k_{OH+HCl}\langle OH\rangle}, \quad (1b)$$

$$\frac{[ClNO_3]}{[HCl]} = \epsilon\,\frac{\langle OH\rangle\langle NO_2\rangle\langle ClO\rangle}{\langle Cl\rangle}\times \frac{k_{ClO+NO_2;M}k_{OH+HCl}}{J_{ClNO_3}\{k_{Cl+CH_4}[CH_4]+k_{Cl+C_2H_6}[C_2H_6]+Y\cdot k_{ClO+OH}\frac{\langle ClO\cdot OH\rangle}{\langle Cl\rangle}+k_{Cl+HO_2}\frac{\langle Cl\cdot HO_2\rangle}{\langle Cl\rangle}\}}, \quad (1c)$$

where [X] denotes the concentration of species without diurnal variation and $\langle X \rangle$ denotes the 24-hour average concentration of species (or of the product of two species) that vary over a day (e.g., $\langle ClO \cdot NO_2 \rangle$ is the 24-hour average of the product of the ClO concentration times the NO_2 concentration). Y denotes the fractional yield of HCl from the reaction ClO + OH, and k and J denote the rate constant and 24-hour average photolysis rate of the indicated reactions, respectively. The concentrations of $ClNO_3$ and HCl are expressed without diurnal variation in the above expressions because, for conditions of MkIV observations considered here, our photochemical model calculations indicate that for altitudes below 28 km the vmr of each species is nearly constant (variations < 10%) over a 24-hour period. The factor ϵ in equation 1a, $\epsilon = \langle ClO \cdot NO_2 \rangle / (\langle ClO \rangle \langle NO_2 \rangle)$, allows further simplification of the steady state relations and the derivation of an analytic expression for the ratio of the principal inorganic chlorine species (i.e., $[ClNO_3]/[HCl]$). In the altitude range 14 to 38 km, values of ϵ calculated by our photochemical model vary between 0.81 and 0.92. *Stimpfle et al.* [1999] have shown that the terms in equation 1a lead to a very close balance between production and loss of $ClNO_3$ during mid-day based on an analysis of simultaneous *in situ* observations of the concentration of $ClNO_3$, ClO, and NO_2 and values for the photolysis rate of $ClNO_3$ found using the same radiative transfer model used here. This result demonstrates that the coupling between $ClNO_3$, ClO, and NO_2 is well understood. For altitudes above 14 km, the term $k_{Cl+CH_4}[CH_4]$ is much larger than $k_{Cl+C_2H_6}[C_2H_6]$. For altitudes below 28 km during polar summer, the production of HCl by the ClO + OH and Cl + HO_2 reactions is small (< 12% of the total HCl production). Therefore equation 1c can be simplified to:

$$\frac{[ClNO_3]}{[HCl]} = \epsilon \frac{\langle OH \rangle \langle NO_2 \rangle}{[CH_4]} \frac{\langle ClO \rangle}{\langle Cl \rangle} \frac{k_{ClO+NO_2;M} k_{OH+HCl}}{J_{ClNO_3} k_{Cl+CH_4}} \tag{2}$$

which is valid between altitudes of 14 and 28 km for polar summer.

Further simplification of equation 2 can be obtained by balancing the primary sources and sinks of Cl and NO, which yields:

$$\frac{\langle ClO \rangle}{\langle Cl \rangle} = \frac{k_{Cl+O_3}[O_3]}{k_{ClO+NO}\langle NO \rangle + k_{ClO+O}\langle O \rangle} \tag{3a}$$

and

$$\frac{\langle NO_2 \rangle}{\langle NO \rangle} = \frac{k_{NO+O_3}[O_3]}{J_{NO_2}} . \tag{3b}$$

For altitudes between 14 and 28 km during polar summer, the value of $k_{ClO+NO}\langle NO \rangle$ exceeds the value of $k_{ClO+O}\langle O \rangle$ by a factor of 60 to 1700. Based on this knowledge and substituting the simplified equation 3a into equation 2 yields:

$$\frac{[ClNO_3]}{[HCl]} = \epsilon\langle OH\rangle \frac{[O_3]}{[CH_4]} \frac{\langle NO_2\rangle}{\langle NO\rangle} \frac{k_{ClO+NO_2;M} k_{OH+HCl} k_{Cl+O_3}}{J_{ClNO_3} k_{Cl+CH_4} k_{ClO+NO}} . \quad (4a)$$

Substituting for the $\langle NO_2\rangle/\langle NO\rangle$ ratio in equation 4a leads to

$$\frac{[ClNO_3]}{[HCl]} = \epsilon\langle OH\rangle \frac{[O_3]^2}{[CH_4]} \frac{k_{ClO+NO_2;M} k_{OH+HCl} k_{Cl+O_3} k_{NO+O_3}}{J_{ClNO_3} J_{NO_2} k_{Cl+CH_4} k_{ClO+NO}} . \quad (4b)$$

Therefore, for altitudes between 14 and 28 km, equation 4b can be expressed as:

$$\frac{[ClNO_3]}{[HCl]} = \alpha \frac{[O_3]^2}{[CH_4]} \quad (5a)$$

where

$$\alpha = \epsilon\langle OH\rangle \frac{k_{ClO+NO_2;M} k_{OH+HCl} k_{Cl+O_3} k_{NO+O_3}}{J_{ClNO_3} J_{NO_2} k_{ClO+NO} k_{Cl+CH_4}} . \quad (5b)$$

As shown below, α is nearly constant between 14 and 28 km and consequently the quantity $[ClNO_3]/[HCl]$ is expected to depend on $[O_3]^2/[CH_4]$.

For altitudes above 28 km a more complicated expression is required to describe the $[ClNO_3]/[HCl]$ ratio. For this region, production of HCl from ClO + OH and Cl + HO_2 is not negligible, the value of $k_{ClO+O}\langle O\rangle$ approaches the value of $k_{ClO+NO}\langle NO\rangle$ (the values of both quantities are nearly equal at 39 km), and $ClNO_3$ exhibits a significant diurnal variation. The complete expression for $\langle ClNO_3\rangle/[HCl]$, valid at all altitudes that are not influenced by heterogeneous reactions involving direct production or loss of HCl, is

$$\frac{\langle ClNO_3\rangle}{[HCl]} = \epsilon \frac{\langle OH\rangle[O_3]}{\frac{k_{ClO+NO}\langle NO\rangle}{\langle NO_2\rangle} + \frac{k_{ClO+O}\langle O\rangle}{\langle NO_2\rangle}} \times \frac{k_{ClO+NO_2;M} k_{OH+HCl} k_{Cl+O_3}}{J'_{ClNO_3}\{k_{Cl+CH_4}[CH_4] + k_{Cl+C_2H_6}[C_2H_6] + Y \cdot k_{ClO+OH} \frac{\langle ClO \cdot OH\rangle}{\langle Cl\rangle} + k_{Cl+HO_2} \frac{\langle Cl \cdot HO_2\rangle}{\langle Cl\rangle}\}} , \quad (6)$$

where $J'_{ClNO_3} = \langle J_{ClNO_3} \cdot ClNO_3\rangle/\langle ClNO_3\rangle$, a correction term to account for the diurnal variation of $ClNO_3$.

Figure 3 illustrates the relationship between MkIV observations at sunrise of the $[ClNO_3]/[HCl]$ ratio and $[O_3]^2/[CH_4]$ for altitudes between 14 and 26 km. The variation of $[ClNO_3]/[HCl]$ at sunrise found by the full photochemical model simulation versus constrained $[O_3]^2/[CH_4]$ is also shown. Finally, the value of the simplified expression for the ratio described by equation 5a, for values of α obtained from the full photochemical model, is displayed. The MkIV measurements in Figure 3 demonstrate that the partitioning of stratospheric $[ClNO_3]$ and [HCl] responds to variations in $[O_3]^2/[CH_4]$ in a manner quite similar to that expected by photochemical theory.

The factor α in equation 5b involves 6 rate constants, J_{ClNO_3}, J_{NO_2}, and the 24-hour average concentration of OH. The near linear relationship in Figure 3 demonstrates that α is nearly constant over this range of altitudes. This occurs because the increase in the concentration of OH with rising altitude is nearly balanced by the decrease in the ratio of kinetic parameters. The good agreement between the measured slope of $[ClNO_3]/[HCl]$ vs. $[O_3]^2/[CH_4]$ and the slope obtained from full photochemical model suggests the various kinetic parameters and the concentrations of OH that enter equation 5b are known fairly well.

The results in Figure 3 alone cannot rule out the possibility that errors in these various parameters cancel in a manner that preserves good agreement between the predicted and observed slope of $[ClNO_3]/[HCl]$ vs. $[O_3]^2/[CH_4]$. However, a variety of other studies that have examined the individual parameters in expression 5b lead to the conclusion that such cancellation of errors is unlikely. An analysis of ER-2 measurements of the concentration of $ClNO_3$ and calculated $[ClNO_3]$ based on simultaneous measurements of ClO and NO_2 concludes that the wavelength and pressure dependence of J_{ClNO_3} is well characterized by the use of the *DeMore et al.* [1997] cross section within our radiative transfer model [*Stimpfle et al.*, 1999]. Another analysis of ER-2 data has concluded that the photolysis rate of NO_2 calculated using our radiative transfer model agrees to better than 8% with values for the photolysis rate of NO_2 measured by the Composition and Photodissociative Flux Measurement (CPFM) instrument and to those inferred from *in situ* observations of NO, NO_2, O_3, ClO, and HO_2 [*Del Negro et al.*, 1999]. The calculated profile of OH using the same photochemical model shows good agreement (differences $< 10\%$) with observations of mid-day OH obtained between 32 and 50 km by the Far Infrared Spectrometer (FIRS-2) near 69°N on 30 April 1997 [*Jucks et al.*, 1998]. Observations of OH near 20 km during POLARIS are typically 15–20% higher than calculated for a model constrained by measured NO_x [*Wennberg et al.*, 1999]; these measurements were made during a period of low aerosol loading and near continuous solar illumination, for which observed NO_x was systematically 20–30% larger than calculated [*Gao et al.*, 1999; *Osterman et al.*, 1999]. Calculated concentrations of OH are nearly identical to those found using standard chemistry if we allow in our photochemical model for changes in the rates of the $OH+NO_2+M \rightarrow HNO_3+M$ [*Dransfield et al.*, 1999] and $OH+HNO_3 \rightarrow NO_3+H_2O$ [*Brown et al.*, 1999] reactions based on recent laboratory observations, which result in accurate simulations of observed NO_x [*Gao et al.*, 1999; *Osterman et al.*, 1999], as well as the speculative missing source for HO_x proposed by *Wennberg et al.* [1999] that leads to better agreement with OH and HO_2. This model results occurs because the increase in calculated OH due to the speculative source is nearly balanced by the decrease in OH driven by the coupling of HO_x and NO_x chemistry. Given the validity of the photochemical model calculation of $\langle OH \rangle$ and the radiative model calculation of J_{ClNO_3}

and J_{NO_2}, we conclude the ratio of the 6 rate constants that enters the expression for $[ClNO_3]/[HCl]$ have been well determined by laboratory experiments [*DeMore et al.*, 1997], and the gas phase production and loss mechanisms for $ClNO_3$ and HCl are well understood.

Figure 3.

2.2.2. MkIV and ER-2 Comparison The measurements of $ClNO_3$, HCl, N_2O, and CCl_y acquired by instruments on board the ER-2 aircraft during POLARIS provide a valuable opportunity for intercomparison of remote and *in situ* observations of chlorine compounds in the Arctic spring-time stratosphere. Figure 4 compares MkIV observations of $ClNO_3$, HCl, and HCl + $ClNO_3$ + HOCl + calculated ClO for the 8 May 1997 balloon flight with *in situ* measurements of $ClNO_3$, HCl, and Cl_y inferred from CCl_y obtained during the 26 April 1997 ER-2 flight of the first phase of POLARIS. We have chosen this ER-2 flight for comparison to the MkIV observations because the range of sampled N_2O was much larger than for other flights during this time period. Chlorine observations are compared by examining their correlation with respect to N_2O to account for the differing dynamical histories of the sampled air masses. Profiles of N_2O obtained over Fairbanks by MkIV and the mean profile of N_2O measured by the ALIAS instrument on board the ER-2 during numerous ascents and descents over Fairbanks showed a bias of 3%, with the *in situ* observations being higher [*Toon et al.*, 1999b]. Based on the observation that profiles of N_2O measured by ALIAS and ATLAS instruments agree to better than 5%, the use of MkIV and ATLAS N_2O as a common tracer for comparison of the other gases should not significantly bias the results. MkIV observations with values of $N_2O > 200$ ppbv were obtained at altitudes below 20 km, the maximum altitude of the ER-2, and are shown as solid symbols to indicate their more direct comparison to the ER-2 measurements. The MkIV balloon measurements were obtained well outside the 1997 Arctic polar vortex [*Toon et al.*, 1999b], while most of the *in situ* observations for vmrs of $N_2O < 200$ ppbv were obtained during an encounter of vortex air near 20 km on 26 April 1997. Since the partitioning of $ClNO_3$ and HCl depends on O_3, CH_4, OH, and various rate constants and photolysis rates, two sets of model calculations are shown in Figure 4: one subject to constraints for measured pressure, temperature, O_3, CH_4, Cl_y, etc. from the MkIV, the other subject to similar constraints from ER-2 instruments.

Figure 4.

The MkIV and ER-2 observations of $ClNO_3$ agree to better than ~16% over the entire range of N_2O, within the 1σ measurement uncertainty of each instrument. The MkIV measurements of HCl tend to be ~9% larger than the *in situ* observations on 26 April for values of N_2O between 200 and 310 ppbv. The difference between the observations of HCl grows to ~25% for N_2O below 160 ppbv. The ER-2 observations at low N_2O were most likely affected by heterogeneous reactions on polar stratospheric clouds (PSCs), and as discussed below, "incomplete recovery" of these air masses following exposure to PSCs is a viable explanation for these differences. The MkIV and

ALIAS observations of HCl, for N_2O between 200 and 310 ppbv, compare extremely well (differences < 1%) for the later ER-2 flights during the first deployment of POLARIS, which were closer to the time of MkIV balloon flight [*Toon et al.*, 1999b]. It is possible that these air masses, outside the vortex, were also recovering from PSC activity as suggested from the observed increase of column HCl and decrease of column $ClNO_3$ during this time [*Toon et al.*, 1999a]. Consequently, the 2 week time difference between the ER-2 and MkIV observations illustrated in Figure 4 may complicate the comparisons of both HCl and $ClNO_3$.

The photochemical steady state simulations shown in Figure 4 are provided to quantify the expected differences in the vmr of HCl and $ClNO_3$ based upon the differences in $[Cl_y]$, $[O_3]$, $[CH_4]$, [OH], temperature, and pressure for air masses sampled by MkIV and the ER-2. The calculated values of [HCl] using the two sets of constraints are in close agreement for all values of N_2O (Figure 4). The different environmental conditions sampled by MkIV and the ER-2 are manifest primarily as differences in calculated photochemical steady state $[ClNO_3]$, for $N_2O < 220$ ppbv. Temperatures below the threshold for formation of PSCs occurred unusually late during the winter/spring of 1996/97 [e.g. *Coy et al.*, 1997]. The apparent overestimation of *in situ* HCl and underestimation of *in situ* $ClNO_3$ by the model is most likely indicative of "incomplete recovery" of the sampled air masses following activation of chlorine by PSCs, since elevated ClO is first converted to $ClNO_3$ (time scale of ~1 month) and more slowly converted to HCl (time scale of ~2 months) [e.g., *Salawitch et al.*, 1988]. This hypothesis is consistent with temporal trends in ground-based column abundances of HCl and $ClNO_3$ measured by MkIV in late April and early May 1997. An analysis of ER-2 measurements of the $[ClNO_3]/[HCl]$ ratio for all of POLARIS reveals that the observed ratio tends to be systematically underestimated by a model constrained by measured OH, opposite to the behavior exhibited on 26 April 1997 and somewhat in disagreement with conclusions based on MkIV observations [P. Voss, manuscript in preparation, 1999]. The anomalous behavior of $[ClNO_3]/[HCl]$ on this day relative to the other ER-2 flights reinforces our notion that these air masses may be "incompletely recovered" from PSC processing. The very good quantitative agreement between the two independent measurements of $ClNO_3$ for $N_2O < 180$ ppbv may therefore be somewhat fortuitous, since the photochemical steady state values of $ClNO_3$ predicted for the air masses sampled by the remote and *in situ* instruments are considerably different.

The sum HCl + $ClNO_3$ + HOCl measured by MkIV plus calculated ClO agrees to within 10% with the estimate of Cl_y based on the total chlorine content of the organic source gases measured by ACATS on the ER-2. Furthermore, the sum HCl + $ClNO_3$ + ClO measured on board the ER-2 is ~92% of Cl_y inferred from organic gases measured by ACATS [*Bonne et al.*, 1999]. These comparisons corroborate the accuracy of the MkIV observations and also demonstrates a single relation, independent of

altitude, describes the variation of Cl_y vs. N_2O to within ~10% for the Arctic summer stratosphere.

Figure 5.

Figure 5 compares the MkIV observations of the vmr of CFC-12, CFC-11, CFC-113, CCl_4, CH_3Cl, and HCFC-22 for the 8 May 1997 balloon flight with *in situ* measurements of the same species acquired by the ACATS instrument and the WAS system on board the ER-2 during POLARIS. The MkIV measurements of CFC-12 and CH_3Cl are in good agreement with the ACATS and WAS observations, with differences significantly smaller (< 8%) than the uncertainties of the measurements (see Sections 1.1 and 1.2). The mean difference for the vmr of CFC-11 measured by MkIV and the ER-2 instruments of 8% is well within the combined uncertainties of the instruments for N_2O > 200 ppbv. However, for N_2O values between 125 and 190 ppbv, the MkIV measurements of CFC-11 are ~36% lower than the ACATS and WAS observations. This difference is likely due to mixing between vortex and extra-vortex air masses, which results in a "flattening out" of the curvature in the non-linear correlation of N_2O vs. CFC-11 observed by MkIV for extra-vortex air. Similar behavior is also apparent for the correlations of other long-lived tracers (CH_4 vs. N_2O, NO_y vs. N_2O) that exhibit a curved relation in extra-vortex air [*Herman et al.*, 1998] and is explored in quantitative detail in a companion study [*Rex et al.*, 1999]

MkIV vmrs of CCl_4 are 10–22% higher than the ER-2 data at all values of N_2O. MkIV retrieves CCl_4 using the ν_3 band at 787–805 cm^{-1} and spectroscopic parameters derived from the temperature dependent absorption cross sections [P. Varanasi and V. Nemtchinov, SUNY–Stony Brook, private communication, 1997]. The 1σ retrieval precision and estimated accuracy of CCl_4 are each 10%. A previous comparison of ATMOS and ER-2 measurements of CCl_4 has illustrated a ~15% bias between the remote and *in situ* observations [*Chang et al.*, 1996], consistent with the discrepancy noted here. The deviation of the MkIV measurements is larger than the estimated uncertainty in the ν_3 band strength and awaits further review of the absorption cross sections and other possible absorbers in the spectral interval.

The average difference for the vmr of HCFC-22 measured by MkIV and WAS is less than 10% with the remote measurements being larger for nearly all values of N_2O. However, the bias is still within the combined uncertainties of both instruments. For N_2O values between 120 and 150 ppbv, the MkIV measurements of HCFC-22 exhibit a "bulge", also observed in ATMOS measurements of mid-latitude lower stratospheric HCFC-22 [*Rinsland et al.*, 1996, Figure 3], and are ~20% higher than the WAS observations. The absence of this feature in the *in situ* data may be due to mixing between vortex and extra-vortex air masses as suggested in the CFC-11 intercomparison.

At low altitudes (N_2O > 200 ppbv) MkIV and *in situ* observations of CFC-113 agree to within the combined measurement uncertainties (21%). However, for N_2O < 200 ppbv the MkIV observations of CFC-113 are much larger (> 50%) than the *in*

situ values, and the differences exceed the combined measurement uncertainties. Since the stratospheric lifetime of CFC-113 is shorter than that of N_2O, it is expected that the CFC-113 vs. N_2O relationship should lie below a linear correlation, as is observed for CFC-11. The failure of the MkIV observations to exhibit this behavior points to an unidentified problem with the CFC-113 retrieval requiring further investigation.

A comparison of the total organic chlorine content (CCl_y) of the atmosphere measured by MkIV, ACATS, and WAS is shown in Figure 6. The remote and *in situ* variations of CCl_y with N_2O obtained are in excellent agreement (mean differences $< 8\%$) for values of $N_2O > 200$ ppbv, the region of the stratosphere near 20 km with little influence from vortex air. The fractional difference grows for smaller values of N_2O below 150 ppbv. However, the differences are less than 20% for all values of N_2O between 90 and 200 ppbv, which are less than the combined uncertainty of the two CCl_y datasets. The aforementioned differences between the MkIV and ER-2 determination of CFC-113 is responsible for the differences in CCl_y exhibited in Figure 6 but do not affect our overall conclusions regarding the budget of stratospheric chlorine.

Figure 6.

3. Conclusions

The near constant value (3.7±0.2 ppbv) of total stratospheric chlorine (organic + inorganic) measured by MkIV FTIR spectrometer (supplemented by ER-2 observations of CH_3CCl_3 vs. CFC-12 and model calculations for ClO) at 65°N during spring and summer 1997 demonstrates that the bulk of stratospheric inorganic chlorine is provided by the decomposition of organic chlorinated species. These observations provide further support to previous studies of other atmospheric regions [e.g., *Zander et al.*, 1992, 1996; *Gunson et al.*, 1994; *Russell et al.*, 1996] that have shown anthropogenic chlorinated organic compounds released at the surface are the primary source of inorganic chlorine available to react with O_3 in the contemporary stratosphere.

Comparison of volume mixing ratios of HCl and $ClNO_3$ observed by MkIV with photochemical steady state model calculations leads us to conclude that the processes that regulate the partitioning of these gases are well understood (differences $< 10\%$ for altitudes below 35 km) under conditions of low aerosol loading and warm temperature such as experienced during POLARIS. Production of HCl from the ClO + OH reaction was determined to play a small role ($< 5\%$) in the partitioning of HCl and $ClNO_3$ for the Arctic spring for altitudes below 28 km and the Arctic summer for altitudes below 32 km, because the concentration of ClO is suppressed by high levels of NO_x. Nonetheless, a model using the *Lipson et al.* [1997] yield for production of HCl agrees more favorably with the observations. Observations obtained by MkIV show that the $[ClNO_3]/[HCl]$ ratio varies with the quantity $[O_3]^2/[CH_4]$ in a manner close to that predicted by photochemical theory.

The MkIV measurements of HCl and $ClNO_3$ exhibit good agreement (differences < 10%) with ER-2 observations of these species obtained by the ALIAS tunable diode laser spectrometer (HCl) and a new Harvard University thermal dissociation resonance fluorescence instrument ($ClNO_3$) for the region of the atmosphere (N_2O > 200 ppbv) where the remote and *in situ* data are directly comparable. Photochemical model simulations are used to guide the interpretation of the comparisons for air masses with N_2O < 200 ppbv: MkIV observations of N_2O < 200 ppbv were obtained for extra-vortex air above 20 km, whereas ER-2 measurements for N_2O < 200 ppbv correspond to air with a strong vortex influence at 20 km. These simulations suggest that some of the differences between MkIV and ER-2 observations of HCl for N_2O < 200 ppbv may be due to "incomplete recovery" of the ER-2 air masses from heterogeneous reactions on polar stratospheric clouds, and the excellent agreement between remote and *in situ* $ClNO_3$ for these values of N_2O may be somewhat fortuitous. The correlation of MkIV Cl_y based on the sum HCl + $ClNO_3$ + HOCl + calculated ClO vs. N_2O agrees to within ~10% with the Cl_y vs. N_2O correlation derived from ACATS gas chromatograph *in situ* observations of organic chlorinated source molecules and N_2O. These comparisons demonstrate that the accuracy and precision estimates of the MkIV retrievals of HCl and $ClNO_3$ are realistic.

Correlations of MkIV observations of CFC-12, CFC-11, and CH_3Cl vs. N_2O exhibit good agreement (differences < 5% for directly comparable air masses) with correlations of these species measured by ACATS and the Whole Air Sampler system on board the ER-2. The MkIV observations of CFC-113 and CCl_4 exhibit larger differences with respect to the *in situ* measurements, which bear further investigation. The correlation of CCl_y (total organic chlorine) vs. N_2O obtained by MkIV and ER-2 instruments agrees to better than 8% for all values of N_2O between 100 and 310 ppbv. The chlorine contents of CCl_4 and CFC-113 make relatively small contributions to CCl_y for the range of N_2O where the remote and *in situ* observations of these species exhibit the largest disagreement. Consequently, the differences noted for these gases do not affect our conclusions regarding the budget of total stratospheric chlorine.

Acknowledgments. The authors wish to thank D.C. Petterson, J.H. Riccio, and R.D. Howe of JPL for their considerable field support during the balloon campaign. We wish to thank P.R. Wamsley and F.L. Moore for help with ACATS measurements. We also wish to thank the NSBF which conducted the balloon launches, flight operations, and recovery of the payload. The May balloon flight was supported by NASDA for ADEOS validation. This work was funded by the NASA Upper Atmosphere Research Program. A portion of this research was performed at the Jet Propulsion Laboratory, California Institute of Technology, under contract with the National Aeronautics and Space Administration.

References

Abbatt, J. P. D., Heterogeneous interactions of BrO and ClO: Evidence for BrO surface recombination and reaction with HSO_3^-/SO_3^{2-}, *Geophys. Res. Lett.*, *23*, 1681–1684, 1996.

Abrams, M. C., M. R. Gunson, L. L. Lowes, C. P. Rinsland, and R. Zander, Pressure sounding of the middle atmosphere from ATMOS solar occultation measurements of atmospheric CO_2 absorption-lines, *Appl. Optics*, *35*, 2810–2820, 1996a.

Abrams, M. C., et al., On the assessment and uncertainty of atmospheric trace gas measurements with high resolution infrared solar occultation spectra from space by the ATMOS experiment, *Geophys. Res. Lett.*, *23*, 2337–2340, 1996b.

Boering, K. A., S. C. Wofsy, B. C. Daube, H. R. Schneider, M. Loewenstein, and J. R. Podolske, Stratospheric mean ages and transport rates from observations of carbon-dioxide and nitrous-oxide, *Science*, *274*, 1340–1343, 1996.

Bonne, G. P., et al., *In situ* measurements of $ClONO_2$: A new thermal dissociation resonance fluorescence instrument on board the NASA ER-2 aircraft, *J. Geophys. Res.*, *this issue*, 1999.

Brown, L. R., M. R. Gunson, R. A. Toth, F. W. Irion, C. P. Rinsland, and A. Goldman, The 1995 atmospheric trace molecule spectroscopy experiment (ATMOS) line list, *Appl. Optics*, *35*, 2828–2848, 1996.

Brown, S. S., R. K. Talukdar, and A. R. Ravishankara, Reconsideration of the rate constant for the reaction of hydroxyl radicals with nitric acid, *J. Phys. Chem.*, *in press*, 1999.

Chance, K., W. A. Traub, D. G. Johnson, K. W. Jucks, P. Ciarpallini, R. A. Stachnik, R. J. Salawitch, and H. A. Michelsen, Simultaneous measurements of stratospheric HO_x, NO_x, and Cl_x: comparison with a photochemical model, *J. Geophys. Res.*, *101*, 9031–9043, 1996.

Chang, A. Y., et al., A comparison of measurements from ATMOS and instruments aboard the ER-2 aircraft: Halogenated gases, *Geophys. Res. Lett.*, *23*, 2393–2396, 1996.

Coy, L., E. R. Nash, and P. A. Newman, Meteorology of the polar vortex - spring 1997, *Geophys. Res. Lett.*, *24*, 2693–2696, 1997.

Del Negro, L. A., et al., Comparison of modeled and observed values of NO_2 and J_{NO_2} during the POLARIS mission, *J. Geophys. Res.*, *this issue*, 1999.

DeMore, W. B., S. P. Sander, D. M. Golden, R. F. Hampson, M. J. Kurylo, C. J. Howard, A. R. Ravishankara, C. E. Kolb, and M. J. Molina, Chemical kinetics and photochemical data for use in stratospheric modeling, *JPL 97-4*, 1997.

Donaldson, D. J., A. R. Ravishankara, and D. R. Hanson, Detailed study of HOCl + HCl $\rightarrow$ Cl_2 + H_2O in sulfuric acid, *J. Phys. Chem. A*, *101*, 4717–4725, 1997.

Dransfield, T. J., K. K. Perkins, N. M. Donahue, J. G. Anderson, M. M. Sprengnether, and K. L. Demerjian, Temperature and pressure dependent kinetics of the gas-phase

reaction of the hydroxyl radical with nitrogen dioxide, *Geophys. Res. Lett., in press*, 1999.

Elkins, J. W., et al., Airborne gas-chromatograph for in-situ measurements of long-lived species in the upper troposphere and lower stratosphere, *Geophys. Res. Lett., 23*, 347–350, 1996.

Gao, R. S., et al., A comparison of observations and model simulations of NO_x/NO_y in the lower stratosphere, *Geophys. Res. Lett., in press*, 1999.

Gunson, M. R., M. C. Abrams, L. L. Lowes, E. Mahieu, R. Zander, C. P. Rinsland, M. K. W. Ko, N. D. Sze, and D. K. Weisenstein, Increase in levels of stratospheric chlorine and fluorine loading between 1985 and 1992, *Geophys. Res. Lett., 21*, 2223–2226, 1994.

Herman, R. L., et al., Tropical entrainment time scales inferred from stratospheric N_2O and CH_4 observations, *Geophys. Res. Lett., 25*, 2781–2784, 1998.

Jaeglé, L., Y. L. Yung, G. C. Toon, B. Sen, and J.-F. Blavier, Balloon observations of organic and inorganic chlorine in the stratosphere: the role of $HClO_4$ production on sulfate aerosols, *Geophys. Res. Lett., 23*, 1749–1752, 1996.

Jucks, K. W., D. G. Johnson, K. V. Chance, W. A. Traub, J. J. Margitan, G. B. Osterman, R. J. Salawitch, and Y. Sasano, Observations of OH, HO_2, H_2O, and O_3 in the upper stratosphere: implications for HO_x photochemistry, *Geophys. Res. Lett., 25*, 3935–3938, 1998.

Kaye, J. A., S. A. Penkett, and F. M. Ormond, eds., *NASA Reference Publication 1339, Report on Concentrations, Lifetimes, and Trends of CFCs, Halons and Related Species*, NASA Office of Missions to Planet Earth, Science Div., Washington, D.C., 1994.

Keating, G. M., and D. F. Young, Interim reference ozone models for the middle atmosphere, in *Handbook for MAP*, edited by K. Labitzke, J. J. Barnett, and B. Edwards, vol. 16, pp. 205–229, SCOSTEP Secretariat, Univ. of Illinois, Urbana, 1985.

Lipson, J. B., M. J. Elrod, T. W. Beiderhase, L. T. Molina, and M. J. Molina, Temperature-dependence of the rate-constant and branching ratio for the OH + ClO reaction, *J. Chem. Soc. Faraday Trans., 93*, 2665–2673, 1997.

Loewenstein, M., J. R. Podolske, K. R. Chan, and S. E. Strahan, Nitrous oxide as a dynamical tracer in the 1987 Airborne Antarctic Ozone Experiment, *J. Geophys. Res., 94*, 11,589–11,598, 1989.

Michelsen, H. A., et al., Stratospheric chlorine partitioning: Constraints from shuttle-borne measurements of [HCl], [$ClNO_3$], and [ClO], *Geophys. Res. Lett., 23*, 2361–2364, 1996.

Minschwaner, K., R. J. Salawitch, and M. B. McElroy, Absorption of solar radiation by O_2: implications for O_3 and lifetimes of N_2O, $CFCl_3$, and CF_2Cl_2, *J. Geophys. Res., 98*, 10,543–10,561, 1993.

Montzka, S. A., J. H. Butler, R. C. Myers, T. M. Thompson, T. H. Swanson, A. D. Clarke,

and J. W. Elkins, Decline in the tropospheric abundance of halogen from halocarbons: implications for stratospheric ozone depletion, *Science*, *272*, 1318–1322, 1996.

Osterman, G. B., B. Sen, G. C. Toon, R. J. Salawitch, J. J. Margitan, J.-F. Blavier, D. W. Fahey, and R. S. Gao, The partitioning of reactive nitrogen species in the summer Arctic stratosphere, *Geophys. Res. Lett., in press*, 1999.

Prather, M. J., Ozone in the upper stratosphere and mesosphere, *J. Geophys. Res.*, *86*, 919–939, 1981.

Ravishankara, A. R., and D. R. Hanson, Differences in the reactivity of type-1 polar stratospheric clouds depending on their phase, *J. Geophys. Res.*, *101*, 3885–3890, 1996.

Rex, M., et al., Subsidence, Mixing and Denitrification of Polars Vortex Air measured during POLARIS, *J. Geophys. Res., this issue*, 1999.

Rinsland, C. P., et al., Trends in OCS, HCN, SF_6, $CHClF_2$ (HCFC-22) in the lower stratosphere from 1985 and 1994 Atmospheric Trace Molecule Spectroscopy experiment measurements near 30°N latitude, *Geophys. Res. Lett.*, *23*, 2349–2352, 1996.

Russell, J. M., M. Z. Luo, R. J. Cicerone, and L. E. Deaver, Satellite confirmation of the dominance of chlorofluorocarbons in the global stratospheric chlorine budget, *Nature*, *379*, 526–529, 1996.

Salawitch, R. J., S. C. Wofsy, and M. B. McElroy, Influence of polar stratospheric clouds on the depletion of Antarctic ozone, *Geophys. Res. Lett.*, *15*, 871–874, 1988.

Salawitch, R. J., et al., The distribution of hydrogen, nitrogen, and chlorine radicals in the lower stratosphere: Implications for changes in O_3 due to emission of NO_y from supersonic aircraft, *Geophys. Res. Lett.*, *21*, 2547–2550, 1994a.

Salawitch, R. J., et al., The diurnal-variation of hydrogen, nitrogen, and chlorine radicals: Implications for the heterogeneous production of HNO_2, *Geophys. Res. Lett.*, *21*, 2551–2554, 1994b.

Schauffler, S. M., L. E. Heidt, W. H. Pollock, T. M. Gilpin, J. F. Vedder, S. Solomon, R. A. Lueb, and E. L. Atlas, Measurements of halogenated organic compounds near the tropical tropopause, *Geophys. Res. Lett.*, *20*, 2567–2570, 1993.

Sen, B., G. Toon, J.-F. Blavier, E. L. Fleming, and C. H. Jackman, Balloon-borne observations of midlatitude fluorine abundance, *J. Geophys. Res.*, *101*, 9045–9054, 1996.

Sen, B., G. C. Toon, G. B. Osterman, J.-F. Blavier, J. J. Margitan, R. J. Salawitch, and G. K. Yue, Measurements of reactive nitrogen in the stratosphere, *J. Geophys. Res.*, *103*, 3571–3585, 1998.

Stimpfle, R., et al., The coupling of $ClONO_2$, ClO and NO_2 in the lower stratosphere from *in situ* observations using the NASA ER-2 aircraft, *J. Geophys. Res., this issue*, 1999.

Thomason, L. W., L. R. Poole, and T. Deshler, A global climatology of stratospheric aerosol surface area density deduced from Stratospheric Aerosol and Gas Experiment II measurements: 1984-1994, *J. Geophys. Res.*, *102*, 8967–8976, 1997.

Toon, G. C., The JPL MkIV interferometer, *Opt. Photonics News*, *2*, 19–21, 1991.

Toon, G. C., J.-F. Blavier, B. Sen, R. J. Salawitch, G. B. Osterman, J. Notholt, M. Rex, C. T. McElroy, and P. Newman, Ground-based observations of Arctic O_3 loss during spring and summer 1997, *J. Geophys. Res.*, *this issue*, 1999a.

Toon, G. C., et al., Comparison of remote and *in situ* observations of atmospheric trace gas profiles, *J. Geophys. Res.*, *this issue*, 1999b.

Wamsley, P. R., et al., Distribution of Halon-1211 in the upper troposphere and lower stratosphere and the 1994 total bromine budget, *J. Geophys. Res.*, *103*, 1513–1526, 1998.

Webster, C. R., R. D. May, C. A. Trimble, R. G. Chave, and J. Kendall, Aircraft (ER-2) laser infrared-absorption spectrometer (ALIAS) for *in situ* stratospheric measurements of HCl, N_2O, CH_4, NO_2, and HNO_3, *Appl. Opt.*, *33*, 454–472, 1994.

Wennberg, P. O., et al., Twilight observations suggest unknown sources of HO_x, *Geophys. Res. Lett.*, *in press*, 1999.

Zander, R., M. R. Gunson, C. B. Farmer, C. P. Rinsland, F. W. Irion, and E. Mahieu, The 1985 chlorine and fluorine inventories in the stratosphere based on ATMOS observations at 30°north latitude, *J. Atmos. Chem.*, *15*, 171–186, 1992.

Zander, R., et al., The 1994 northern midlatitude budget of stratospheric chlorine derived from ATMOS/ATLAS-3 observations, *Geophys. Res. Lett.*, *23*, 2357–2360, 1996.

Zhang, R. Y., M. T. Leu, and L. F. Keyser, Heterogeneous chemistry of HONO on liquid sulfuric-acid - a new mechanism of chlorine activation on stratospheric sulfate aerosols, *J. Phys. Chem.*, *100*, 339–345, 1996.

B. Sen, Jet Propulsion Laboratory, California Institute of Technology, MS 183-601, 4800 Oak Grove Drive, Pasadena, CA 91109. email: bhaswar.sen@jpl.nasa.gov.
[06-04-1999@14:14, Distrib.Ver. 3]

Received January 1, 2000; revised January 1, 2000; accepted January 1, 2000.

This manuscript was prepared with AGU's LaTeX macros v4, with the extension package 'AGU++' by P. W. Daly, version 1.5f from 1998/07/16.

Figure Captions

Figure 1. Budget of organic chlorine (CCl_y = 2·CFC-12 + 3·CFC-11 + 3·CFC-113 + 4·CCl_4 + CH_3Cl + HCFC-22 + 3·CH_3CCl_3), inorganic chlorine (Cl_y = HCl + $ClNO_3$ + HOCl + ClO) and their sum (Cl_{TOT}) between 9 and 38 km on 8 May 1997. All gases were measured by MkIV at sunrise, except CH_3CCl_3, for which the vmr profile was estimated from MkIV CFC-12 based on a relation derived from ACATS measurements, and except ClO, for which a vmr profile at sunrise was calculated using standard chemistry [*DeMore et al.*, 1997] and the ~6% yield of HCl from ClO+OH reported by *Lipson et al.* [1997]. Observations of CCl_y and Cl_y have been displaced in altitude slightly for visual clarity. Error bars represent 1σ measurement precision in this and other figures (see Section 1.1).

Figure 2. MkIV observations and calculations of vmr profiles of HCl and $ClNO_3$, as indicated, at 65°N during sunrise on 8 May and during payload ascent on 8 July 1997. The calculations are shown for two different yields of HCl from ClO + OH: 0% (dashed line) and the ~6% (solid line) yield measured by *Lipson et al.* [1997].

Figure 3. Measured and calculated values of $[ClNO_3]/[HCl]$ and $[O_3]^2/[CH_4]$ during sunrise on 8 May 1997. The full photochemical calculations (solid line) use reaction rates and absorption cross sections [*DeMore et al.*, 1997] plus the *Lipson et al.* [1997] temperature dependent yield of HCl from ClO + OH and are constrained by MkIV measurements of pressure, temperature, O_3, H_2O, CH_4, C_2H_6, HCl + $ClNO_3$ + HOCl, and NO_y as well as SAGE II monthly zonal mean aerosol surface area. The dashed line shows the value of the simplified expression for $[ClNO_3]/[HCl]$ (equation 5a) based on photolysis rates and $\langle OH \rangle$ from the photochemical model and rate constants from *DeMore et al.* [1997].

Figure 4. The volume mixing ratio (vmr) of HCl and $ClNO_3$ versus N_2O observed by MkIV for the 8 May 1997 balloon flight, as indicated (solid symbols designate observations obtained at altitudes of 20 km and below). *In situ* measurements of HCl and $ClNO_3$ versus N_2O obtained near 20 km by instruments on board the ER-2 aircraft on 26 April 1997. Calculated values of HCl and $ClNO_3$ (solid lines) assuming photochemical steady state are shown for both MkIV and ER-2 constraints for long-lived precursors, latitude, temperature, etc. The sum HCl + $ClNO_3$ + HOCl measured by MkIV plus calculated ClO is compared to the estimates of Cl_y from *in situ* observations of CCl_y by the ACATS instrument on board the ER-2.

Figure 5. Correlations of volume mixing ratio profiles of CFC-12, CFC-11, CFC-113, CCl_4, CH_3Cl, and HCFC-22 versus N_2O measured remotely by MkIV (diamonds) and *in situ* by ACATS (green dots) and WAS (red crosses) on board the ER-2. MkIV sunrise balloon measurements were made on 970508; the ACATS and WAS observations were obtained during the first deployment of POLARIS (970422–970513).

Figure 6. Correlations of volume mixing ratio profiles of CCl_y (= 2·CFC-12 + 3·CFC-11 + 3·CFC-113 + 4·CCl_4 + CH_3Cl + HCFC-22 + 3·CH_3CCl_3) versus N_2O measured by MkIV, ACATS, and WAS (as indicated). The mixing ratio of CH_3CCl_3 needed for the MkIV estimate of CCl_y was found from the MkIV observation of CFC-12, using a relation based on ACATS measurements.

Figures

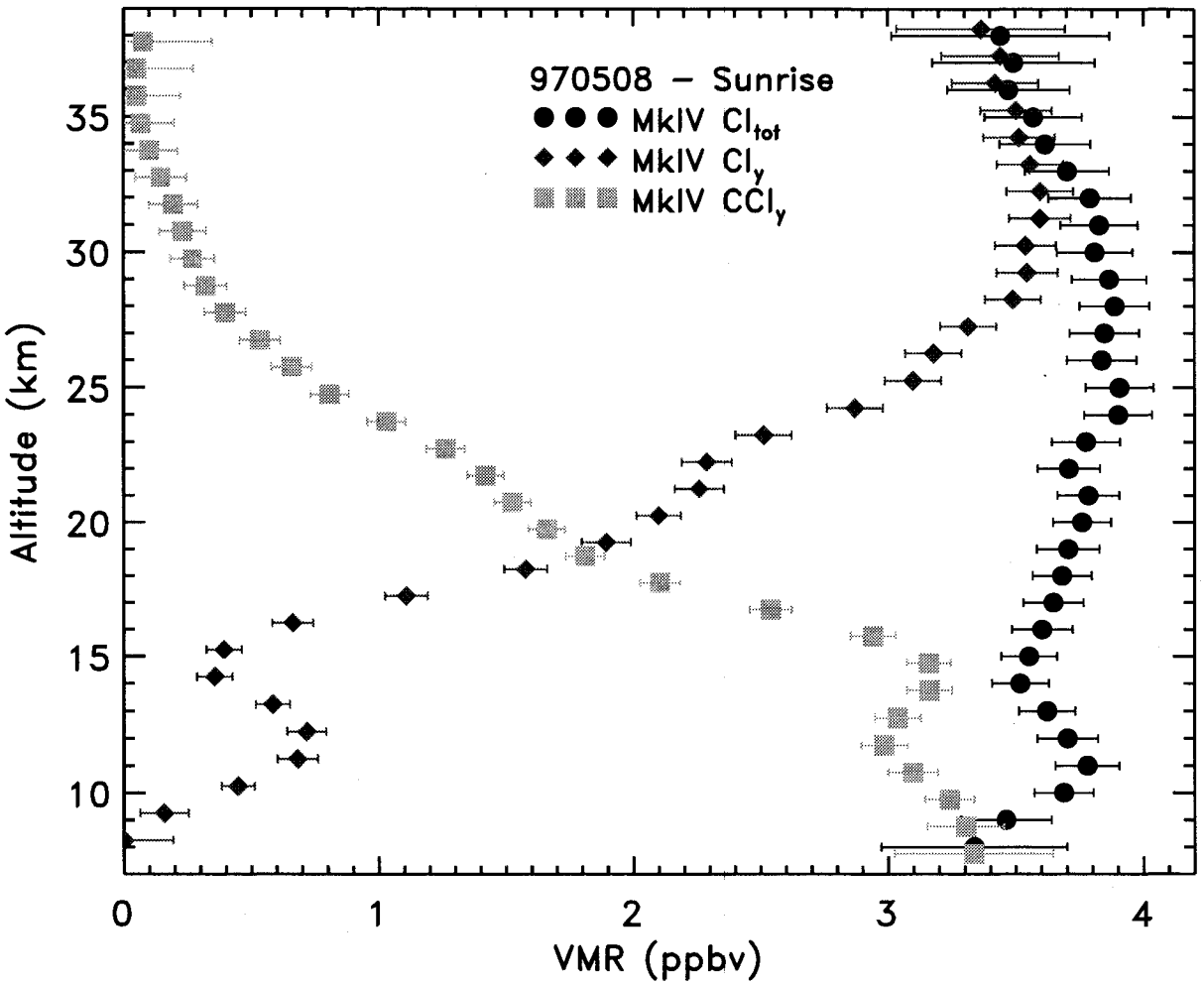

Figure 1. Budget of organic chlorine (CCl_y = 2·CFC-12 + 3·CFC-11 + 3·CFC-113 + 4·CCl_4 + CH_3Cl + HCFC-22 + 3·CH_3CCl_3), inorganic chlorine (Cl_y = HCl + $ClNO_3$ + HOCl + ClO) and their sum (Cl_{TOT}) between 9 and 38 km on 8 May 1997. All gases were measured by MkIV at sunrise, except CH_3CCl_3, for which the vmr profile was estimated from MkIV CFC-12 based on a relation derived from ACATS measurements, and except ClO, for which a vmr profile at sunrise was calculated using standard chemistry [*DeMore et al.*, 1997] and the ~6% yield of HCl from ClO+OH reported by *Lipson et al.* [1997]. Observations of CCl_y and Cl_y have been displaced in altitude slightly for visual clarity. Error bars represent 1σ measurement precision in this and other figures (see Section 1.1).

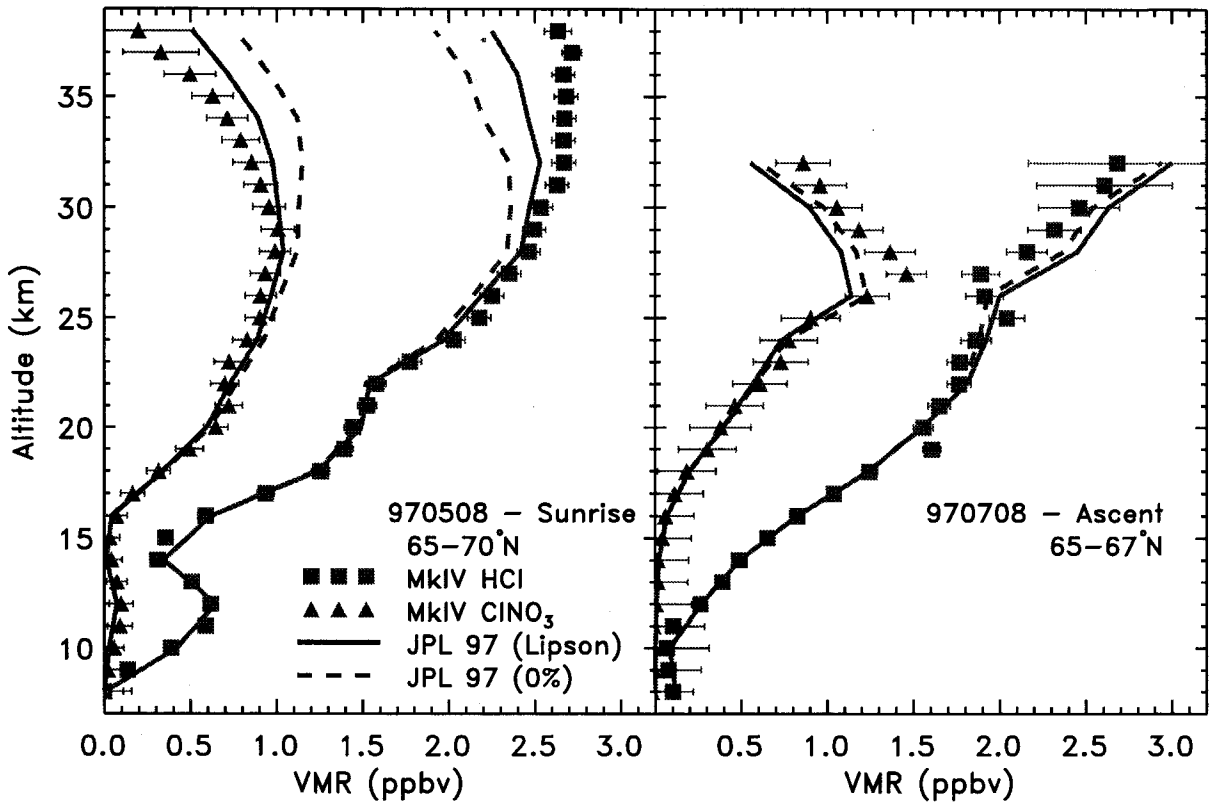

Figure 2. MkIV observations and calculations of vmr profiles of HCl and $ClNO_3$, as indicated, at 65°N during sunrise on 8 May and during payload ascent on 8 July 1997. The calculations are shown for two different yields of HCl from ClO + OH: 0% (dashed line) and the ~6% (solid line) yield measured by *Lipson et al.* [1997].

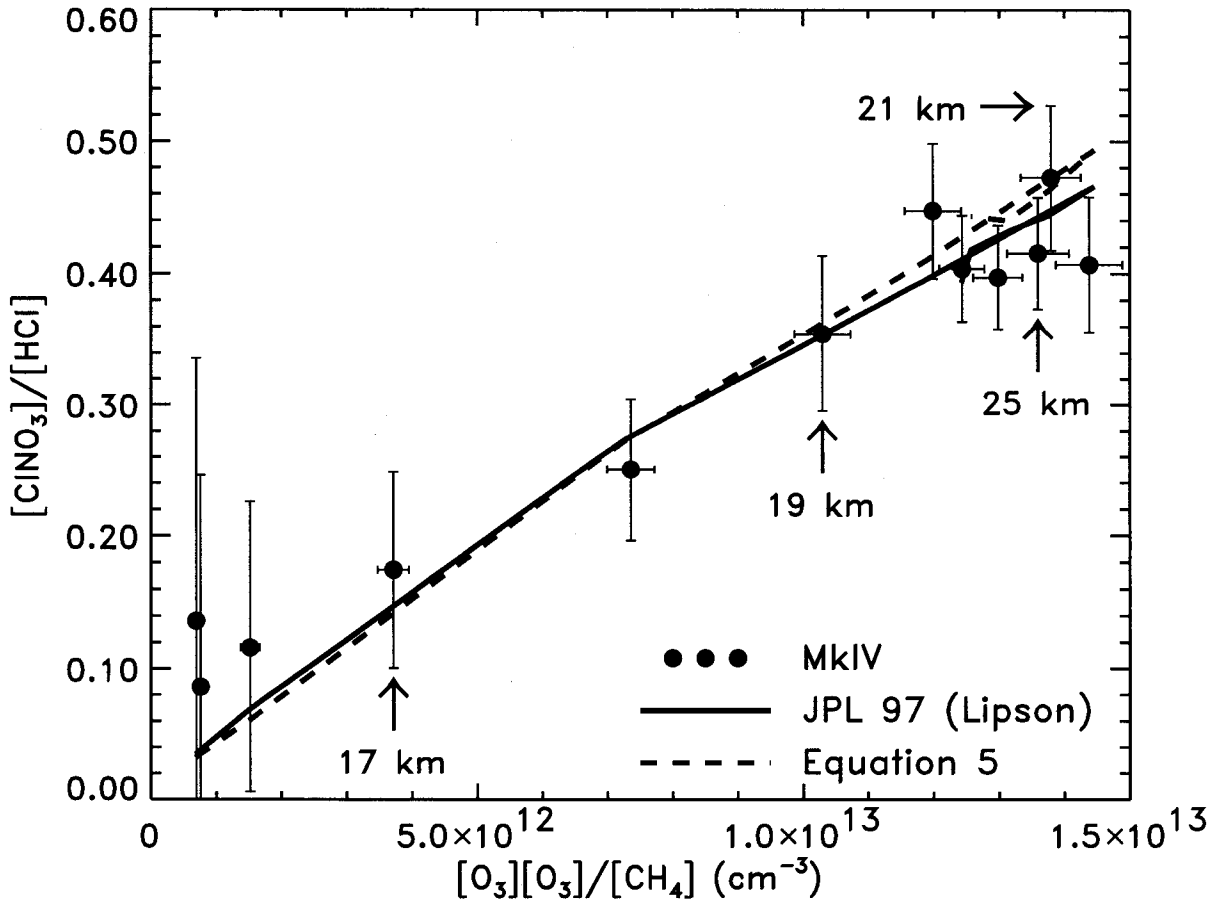

Figure 3. Measured and calculated values of $[ClNO_3]/[HCl]$ and $[O_3]^2/[CH_4]$ during sunrise on 8 May 1997. The full photochemical calculations (solid line) use reaction rates and absorption cross sections [*DeMore et al.*, 1997] plus the *Lipson et al.* [1997] temperature dependent yield of HCl from ClO + OH and are constrained by MkIV measurements of pressure, temperature, O_3, H_2O, CH_4, C_2H_6, HCl + $ClNO_3$ + HOCl, and NO_y as well as SAGE II monthly zonal mean aerosol surface area. The dashed line shows the value of the simplified expression for $[ClNO_3]/[HCl]$ (equation 5a) based on photolysis rates and $\langle OH \rangle$ from the photochemical model and rate constants from *DeMore et al.* [1997].

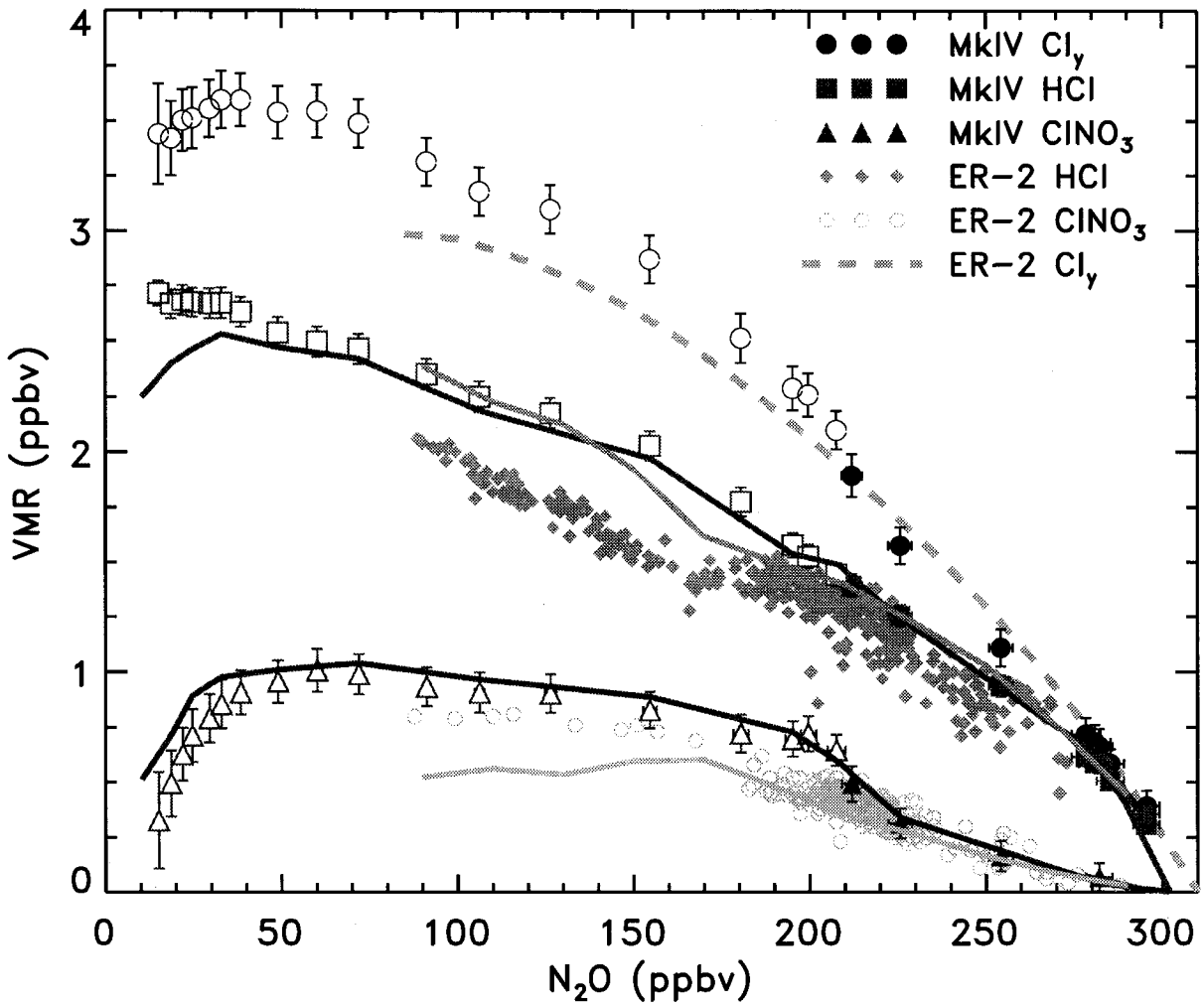

Figure 4. The volume mixing ratio (vmr) of HCl and $ClNO_3$ versus N_2O observed by MkIV for the 8 May 1997 balloon flight, as indicated (solid symbols designate observations obtained at altitudes of 20 km and below). *In situ* measurements of HCl and $ClNO_3$ versus N_2O obtained near 20 km by instruments on board the ER-2 aircraft on 26 April 1997. Calculated values of HCl and $ClNO_3$ (solid lines) assuming photochemical steady state are shown for both MkIV and ER-2 constraints for long-lived precursors, latitude, temperature, etc. The sum HCl + $ClNO_3$ + HOCl measured by MkIV plus calculated ClO is compared to the estimates of Cl_y from *in situ* observations of CCl_y by the ACATS instrument on board the ER-2.

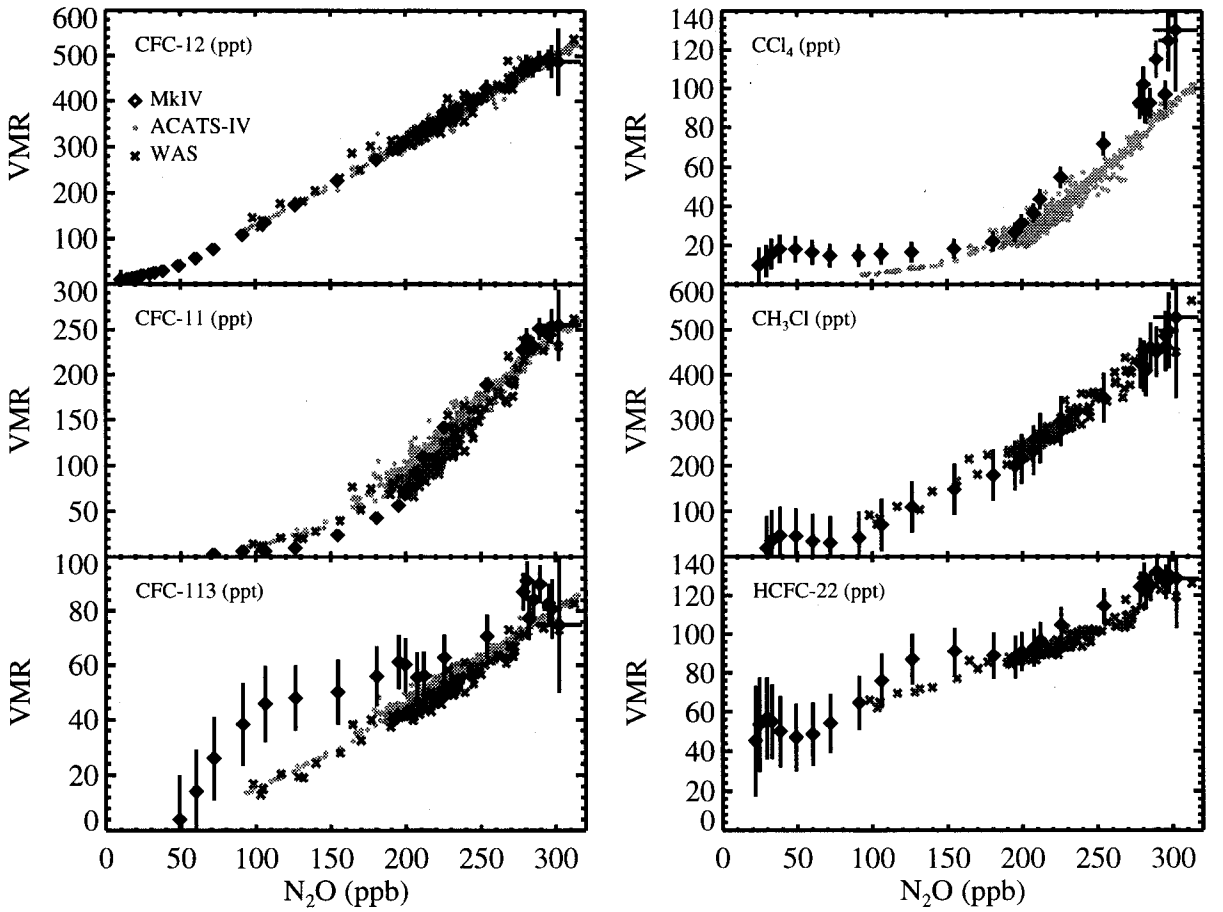

Figure 5. Correlations of volume mixing ratio profiles of CFC-12, CFC-11, CFC-113, CCl_4, CH_3Cl, and HCFC-22 versus N_2O measured remotely by MkIV (diamonds) and *in situ* by ACATS (green dots) and WAS (red crosses) on board the ER-2. MkIV sunrise balloon measurements were made on 970508; the ACATS and WAS observations were obtained during the first deployment of POLARIS (970422–970513).

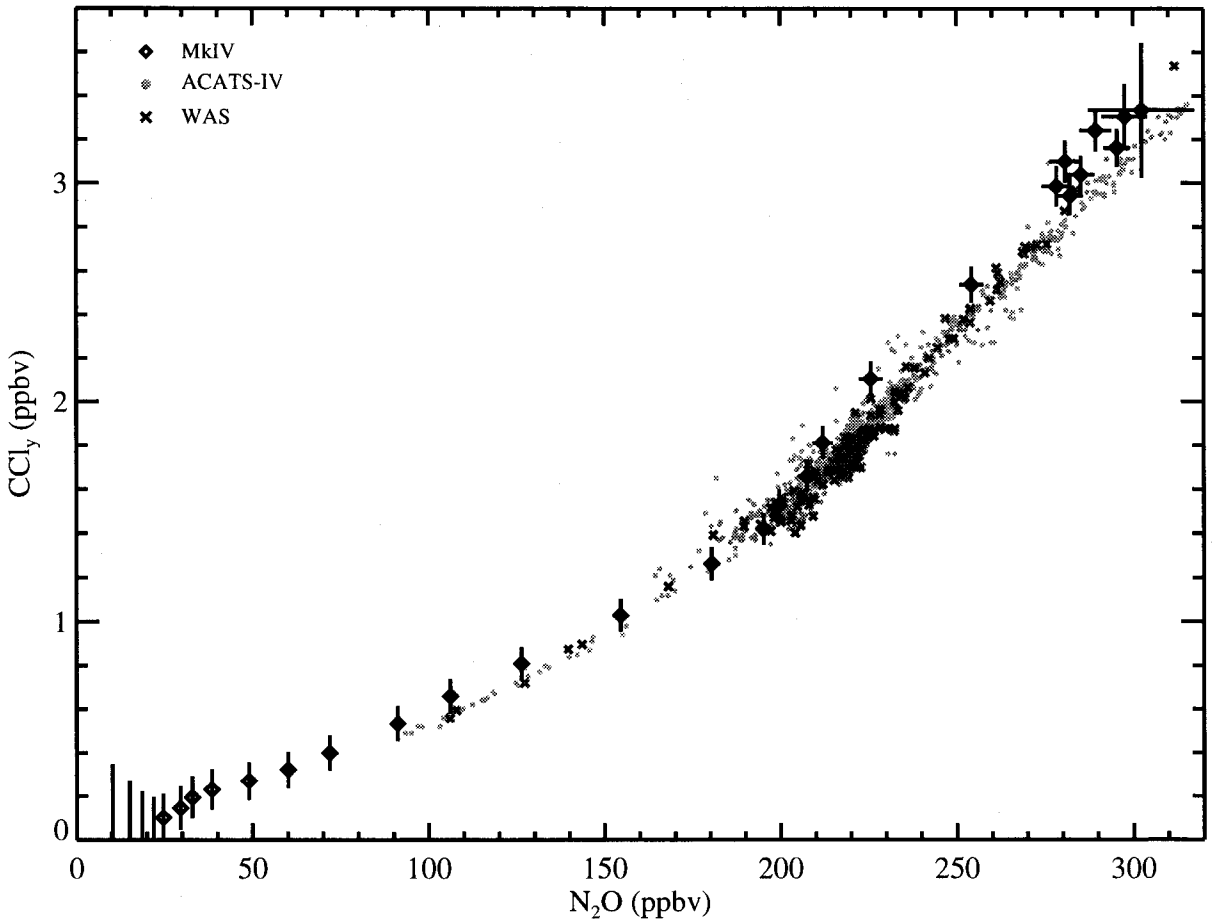

Figure 6. Correlations of volume mixing ratio profiles of CCl_y (= 2·CFC-12 + 3·CFC-11 + 3·CFC-113 + 4·CCl_4 + CH_3Cl + HCFC-22 + 3·CH_3CCl_3) versus N_2O measured by MkIV, ACATS, and WAS (as indicated). The mixing ratio of CH_3CCl_3 needed for the MkIV estimate of CCl_y was found from the MkIV observation of CFC-12, using a relation based on ACATS measurements.